Chen et al. *EPJ Data Science* (2024) 13:30
https://doi.org/10.1140/epjds/s13688-024-00471-4

EPJ Data Science
a SpringerOpen Journal

RESEARCH Open Access

Scaling law of real traffic jams under varying travel demand

Rui Chen[1], Yuming Lin[1*], Huan Yan[1], Jiazhen Liu[1], Yu Liu[1] and Yong Li[1]

*Correspondence:
linyuming9@mail.tsinghua.edu.cn
[1]Department of Electronic Engineering, Tsinghua University, Haidian District, Beijing, China

Abstract

The escalation of urban traffic congestion has reached a critical extent due to rapid urbanization, capturing considerable attention within urban science and transportation research. Although preceding studies have validated the scale-free distributions in spatio-temporal congestion clusters across cities, the influence of travel demand on that distribution has yet to be explored. Using a unique traffic dataset during the COVID-19 pandemic in Shanghai 2022, we present empirical evidence that travel demand plays a pivotal role in shaping the scaling laws of traffic congestion. We uncover a noteworthy negative linear correlation between the travel demand and the traffic resilience represented by scaling exponents of congestion cluster size and recovery duration. Additionally, we reveal that travel demand broadly dominates the scale of congestion in the form of scaling laws, including the aggregated volume of congestion clusters, the number of congestion clusters, and the number of congested roads. Subsequent micro-level analysis of congestion propagation also unveils that cascade diffusion determines the demand sensitivity of congestion, while other intrinsic components, namely spontaneous generation and dissipation, are rather stable. Our findings of traffic congestion under diverse travel demand can profoundly enrich our understanding of the scale-free nature of traffic congestion and provide insights into internal mechanisms of congestion propagation.

Keywords: Traffic congestion; Travel demand; Scaling law; Complex systems

1 Introduction

Traffic congestion is characterized by slower vehicle speeds, longer trip times and increased queuing of vehicles, often occurring when travel demand exceeds the road capacity [1]. In 2022, the total cost of traffic congestion was over $81 billion in the US and £9.5 billion in the UK [2], making it a severe problem hindering urban development. Studies have shown that under various internal or external disturbances, minor congestion can potentially evolve into large-scale cascading reactions similar to a domino effect [3–5], with unpredictable and severe consequences. In light of this, it is highly crucial to explore factors that affect traffic congestion and understand its intrinsic characteristics, which can contribute significantly to enhancing traffic planning [6, 7] and traffic management [8, 9].

There have been adequate studies that approached the issue of congestion from the perspectives of demand and supply, focusing on factors such as travel demand [10–15], road network supply [16–19], and network topology [20–23]. Other studies have examined how resident travel patterns and transportation mode choices may influence the development of congestion [24–26], or how the socio-economic attributes of cities, like population density [27–29] and land area [30–34], can shape the congestion. Besides, external factors such as climate conditions also play a role in traffic congestion [35–37]. However, these studies primarily employ simulation or machine learning methods, which exhibit limitations in gaining insight into the fundamental principles governing urban traffic congestion.

To investigate further mechanisms governing urban traffic congestion in real-life scenes, more researchers have recently turned to physical models from empirical data. The percolation theory is widely used to model traffic congestion, providing valuable insight through the analysis of critical percolation threshold [1, 38, 39]. The framework of urban scaling law [40] is also promising since the scale-free distribution has been observed in many urban subsystems [41–43], as well as in the congestion percolation transition [44, 45]. The concept reveals the self-similarity of a system, wherein the system exhibits similar behavioral patterns at different spatial or temporal scales [46, 47]. This self-similarity means rules on different spatial regions and time scales follow the same statistic, which has wide-ranging applications in exploring nonlinear behaviors and self-organizing phenomena in complex systems [41, 48–50]. In traffic congestion propagation within road networks, jammed clusters can range from an entire area to a small section of road, lasting from minutes to hours. And the urban scaling law can unveil their inherent nature by studying their basic variables: cluster size for their spatial size and duration for their temporal size [51–54]. One of the critical research by Zhang et al. verified that the distribution of congestion cluster size and duration shows a scale-free property, independent of microscopic details [53]. When the distribution of these metrics follows a power-law pattern, it indicates the presence of similar congestion phenomena at various scales, rather than being isolated incidents [52, 55]. Furthermore, this pattern often reflects the self-organizing nature and nonlinear behavior within complex systems [56, 57]. Therefore, by identifying this power-law distribution, we can gain a better understanding of the dynamic characteristics of traffic networks and how congestion emerges and spreads within the road networks. This, in turn, facilitates more accurate congestion prediction and management, enhances the efficiency of road networks, and supports the development of more effective traffic policies.

However, despite Zhang et al.'s observations [53] claim that the power-law exponents of size and duration distributions are stable on different workdays in different cities, there are still some critical issues that need to be explored. Firstly, the study mentioned a higher exponent during the significantly decreased travel demand but did not further analyze possible influence from demand. Furthermore, the study primarily focused on the overall distribution of congestion and did not delve into the propagation of congestion, which is critical for understanding possible cascading diffusion under strong traffic demand [58]. Based on these considerations, our study aims to fill this gap by focusing primarily on the scale-free property of traffic congestion and its propagation characteristics in different travel demand levels.

Studying the impact of traffic demand on congestion may face challenges from the relative stability of travel demand in the city. Albeit there are some fluctuations in traffic volumes between weekends, holidays, and weekdays [53], the intensity of these variations is often insignificant. While the long-term variations are usually accompanied by changes in land use and urban morphology [59], making direct comparisons imprudent. The outbreak of COVID-19 and the corresponding lockdown, as a black swan event [60, 61], have provided us with excellent empirical data. During the pandemic of COVID-19, travel demand has undergone tremendous changes in the same urban setting, making it a natural experiment to study the patterns and variations of traffic congestion in different travel demands.

We conducted the research using real traffic data of Shanghai City from March 1st, 2022, to July 1st, 2022, covering an entire period of the pandemic cycle with dramatically decreased and slowly recovered travel demand. Our result shows that the traffic resilience, described by the distribution exponents of congestion cluster size and recovery duration [53], linearly decreases as travel demand increases. Besides the exponents of distributions, travel demand also brings about a significant impact on the scale of congestion, with a sub-linear scaling relation to the aggregate volume and a modified scaling-like relation to the number of congestion clusters. In microscopic consecutive periods, our results suggest that rising demand will lead to a sharp worsening of congestion, demonstrated by the super-linear scaling relation between the number of congested roads and vehicles on the roads. Subsequent analysis demonstrates that cascade diffusion dominates such sharp worsening, while other propagation components like spontaneous generation and dissipation are rather stable. Our results show the critical role of travel demand, enable better prediction and management of urban traffic and subsequently improve traffic efficiency and sustainability.

2 Results

2.1 Scale-free distributions of traffic congestion cluster

We conducted our research using real traffic data from Shanghai covering the pandemic period from March 1st, 2022 to July 1st, 2022. Shanghai is one of the largest cities in China, characterized by an intricate road network and substantial traffic flow. From March 28th to June 1st, 2022, Shanghai implemented a lockdown policy to stop the pandemic [62], including suspension of the public transportation system and strict traffic permit control for private vehicles. The fluctuations in travel demand resulting from the pandemic and policies facilitated the availability of non-routine large-scale traffic data, providing us with real traffic data under varying travel demands.

Considering congestion in urban areas often forms clusters through propagation, we first construct spatiotemporal congestion clusters [53] for subsequent analysis. Specifically, the road network of Shanghai is abstracted into a directed graph where each node represents a road segment, edges represent the adjacency relationships between road segments, and the direction of edges aligns with the direction of traffic flow. Therefore, congestion can be viewed as a spatiotemporal cluster on the graph, where all spatial or temporal connected congested road segments are assigned to the same jammed cluster, constructing multiple spatiotemporal jammed clusters within the road network of Shanghai cross time (see Additional file 1, Sect. 2 for the details). All the red links within the shaded area of Fig. 1A belong to the same cluster, an example of a spatiotemporal jammed cluster. Note that, when a jammed cluster splits into two or more subgraphs at a certain time, all

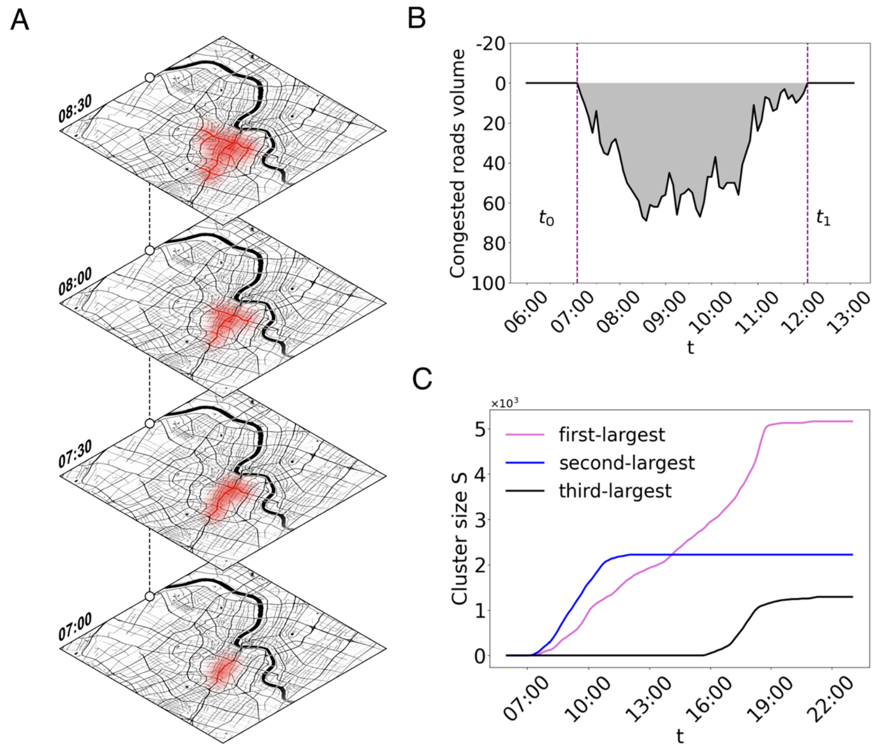

Figure 1 Spatiotemporal jammed clusters in Shanghai. (A) Illustration of the evolution of a jammed cluster in Shanghai. Red links represent congested roads. All red links in the shadow belong to the same jammed cluster. (B) The number of congested roads of the second largest jammed cluster on March 1st, 2022 in Shanghai, where the y-axis is reversed to put the larger number at a lower location. The gray area is the size of the spatiotemporal jammed cluster (S) shown in red in A. The timespan between t_0 and t_1 represents its recovery time ($T = t_1 - t_0$). (C) The cluster size (S) of the first, second, and third largest jammed clusters on March 1st, 2022 in Shanghai as a function of time

nodes within all subgraphs still belong to the same cluster since they are temporally connected. This construction of jammed clusters intuitively reflects the propagation of traffic congestion in both time and space, laying the foundation for subsequent analysis.

The schematic representation of the second-largest jammed cluster in Shanghai on March 1st is depicted in Fig. 1B. The horizontal axis represents time, and the vertical axis depicts the number of congested road segments within this cluster at each time t. To illustrate that the congestion is a deduction of traffic capacity and to align with the resilience triangular, the y-axis is reversed to put the larger number at a lower location. The recovery duration T of the jammed cluster is defined as the duration between the first congested road segment of this cluster occurring t_0 and the last congested segment dissipating t_1. Furthermore, the shaded region in Fig. 1B represents the temporal accumulation of congested road segments, defined as the cluster size S. The specific jammed cluster gradually increases to approximately 60 and then recovers to zero, leading to an accumulative S that speeds up and then slows down. The temporal evolution of the size S of the three largest jammed clusters on March 1st is shown in Fig. 1C, showing distinct characteristics. The largest jammed cluster in pink persists throughout the day and dissipates completely after 18:00. While the jammed cluster in blue emerges during the morning rush hour, and the jammed cluster in black develops during the evening rush hour.

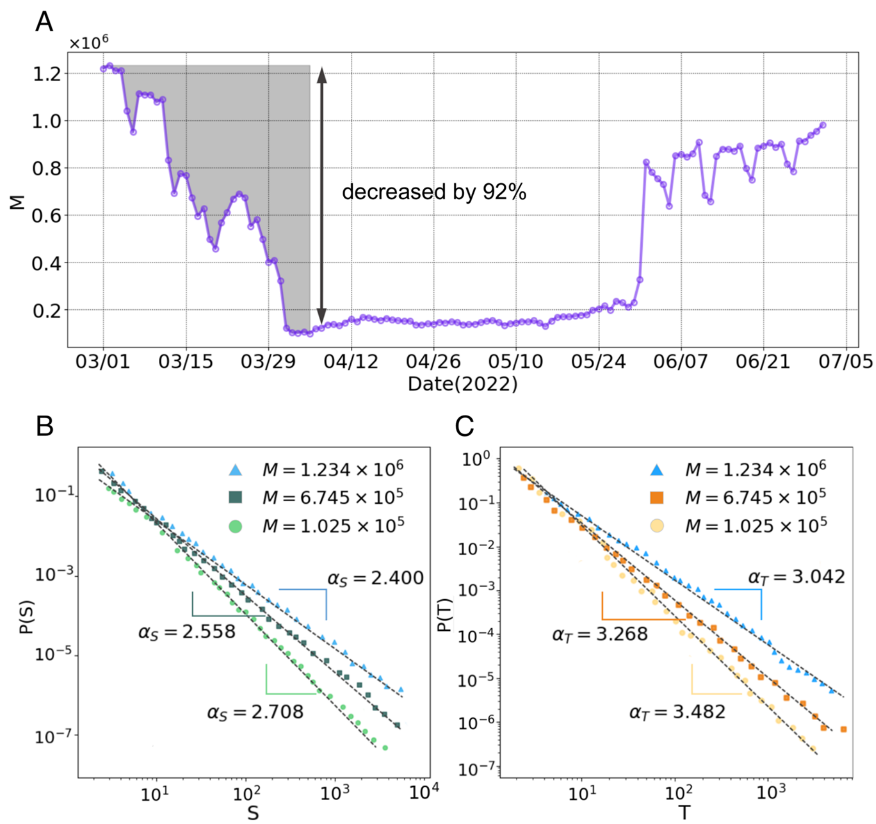

Figure 2 Illustration of scale-free distributions of jammed clusters under different total travel demand. (A) The total travel demand in Shanghai as a function of date. (B) The distribution of the jammed cluster size *S* under different total travel demand *M*. (C) The distribution of recovery duration *T* under different total travel demand *M*

To further explore the impact of travel demand, we utilize the number of origin-destination (OD) pairs, denoted as M, as a representation of daily travel demand (Fig. 2A). It can be observed that following the outbreak of the pandemic, the travel demand in Shanghai experienced a significant decrease of 92%, remained at a lower level during the lockdown, and gradually recovered to a near pre-pandemic level after the policy was lifted. Under such dramatically varying travel demand in a relatively short period, our dataset can reflect the impact of travel demand on the traffic road system.

To further understand the spatial and temporal characteristics of a single jammed cluster, we look into its size S and duration T. The S captures how spatially the congestion ranges and the T captures how temporally it lasts. Considering that a jammed cluster contains many stochastic factors, it is more important to examine their distribution on the variation of traffic demand [44, 45, 53]. As shown in Fig. 2B,C, we observe significant variations in both size and recovery duration of jammed clusters, which aligns with previous research. We confirm that both cluster size S and recovery duration T follow a power-law distribution, specifically

$$p(S) \sim S^{-\alpha_S} \quad \text{and} \quad p(T) \sim T^{-\alpha_T} (\alpha_S, \alpha_T > 0), \tag{1}$$

with parameters $\alpha_S \in [2.40, 2.71]$ and $\alpha_T \in [3.04, 3.48]$ respectively. The results are very close to the 2.3 and 3.1 in Beijing and Shenzhen reported by Zhang et al. [53]

The ubiquity of scale-free distributions across different days suggests that despite varying demand, traffic jams exhibit the same self-organizing mechanisms. However, it is equally noteworthy that scaling exponents α_S and α_T, representing traffic resilience, exhibit significant differences across travel demand. During periods of high travel demand, the scaling exponents are smaller. Whereas, during periods of low travel demand, the scaling exponent of the distribution is larger (Fig. 2B,C). Note that smaller α_S and α_T mean more prevalent larger jammed clusters and longer recovery duration, and the congestion clusters are less vulnerable and harder to deal with. Therefore, it is reasonable to conclude that higher travel demand is related to worse traffic congestion.

2.2 Travel demand and scaling exponents of congestion clusters

Since the scaling exponents capture the full picture of congestion, we further investigate the correlation between the scaling exponents and the daily travel demand. As depicted in Fig. 3A,B, a strong negative linear correlation exists between the scaling exponents and the travel demand M, which holds true for both cluster size α_S (Fig. 3A) and duration α_T (Fig. 3B):

$$\begin{aligned} \alpha_S &= 2.7134 - 2.485 \times 10^{-7} M \quad \left(R^2 = 0.91\right), \\ \alpha_T &= 3.5078 - 3.844 \times 10^{-7} M \quad \left(R^2 = 0.94\right). \end{aligned} \tag{2}$$

These findings indicate that daily travel demand directly influences the magnitude of congestion distributions. Specifically, an increase of one unit in travel demand results in a corresponding decrease of 2.485×10^{-7} in the scaling exponent of jammed cluster size. Likewise, with every unit increase in travel demand, we observe a decline by 3.844×10^{-7} in the scaling exponent for recovery duration. This means that the power-law exponent is not stable as reported before [53], and the variation can be observed in the case of large changes in travel demand.

Since the travel demand M represents a daily variation, we further investigate its relationship with the total congestion size S_{total}, which is defined as the sum of all congestion cluster size S and represents a cumulative measure of daily congestion. As demonstrated in Fig. 3C, the S_{total} exhibits a power-law growth with respect to M, following the relationship:

$$S_{\text{total}} = S_0 \cdot M^{\lambda}, \tag{3}$$

where $S_0 = 1.00$, $\lambda = 0.78$ ($R^2 = 0.94$, 95% $CI = [0.75, 0.81]$). The observed sub-linear scaling exponent $\lambda < 1$ suggests the growth rate of congestion is relatively slower than the corresponding increase of demand, implying the possible existence of self-organizing properties within the traffic network system. When travel demand grows, for instance, traffic flow can be distributed throughout various road segments and time periods by changes to routes and timetables, resulting in a comparatively slower growth in congestion.

Furthermore, by leveraging the quantitative relationship between M, α_S and S_{total}, we can mathematically derive the relationship between the number of jammed clusters N

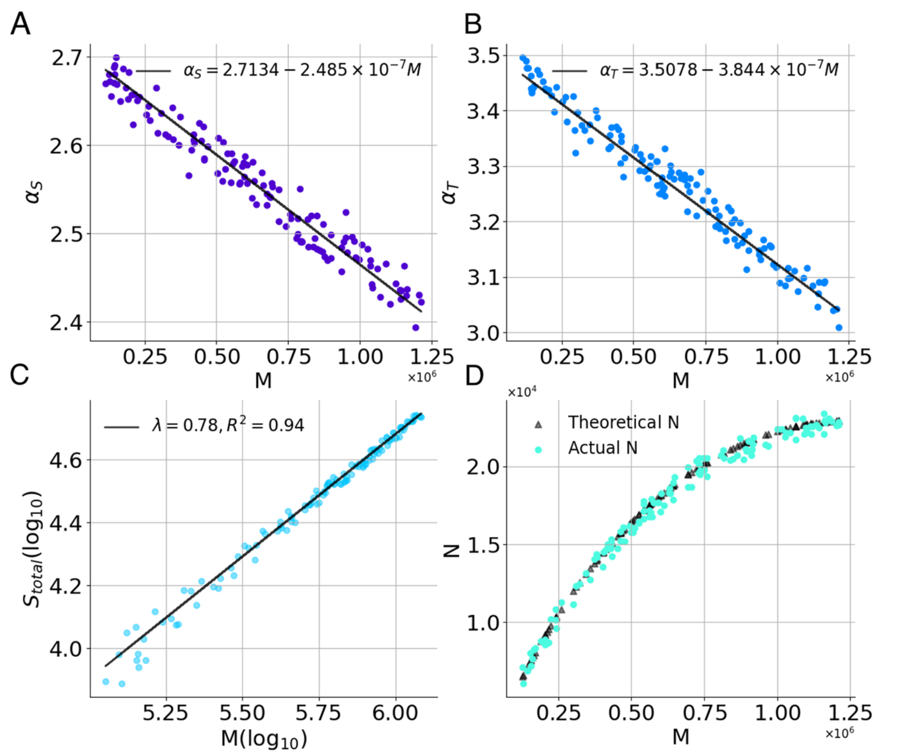

Figure 3 Correlation between the power-law exponent of the spatial and temporal distribution of jammed clusters and aggregate travel demand. (A) Correlation between the power-law exponent of the jammed cluster size α_S and the aggregate travel demand *M*. (B) Correlation between the power-law exponent of the jammed cluster size α_T and the aggregate travel demand *M*. (C) The scaling law of aggregate cluster size S_{total} and aggregate travel demand *M*. (D) The number of jammed clusters under different travel demand. The theoretical values of *N* are calculated using Eq. (6)

and travel demand M. Assuming the size of a single cluster is denoted by S, the value of summing up all daily values of S_{total} can be represented as

$$S_{\text{total}} = N \cdot \mathbb{E}[S], \tag{4}$$

where $\mathbb{E}[S]$ represents the expected value of a single cluster size. Given the power-law probability distribution of $p(S) \sim S^{-\alpha_S}$, we have

$$\mathbb{E}[S] = \int_1^{\infty} S \cdot p(S) \cdot \mathrm{d}S = \frac{1}{\alpha_S - 2}, \quad \alpha_S > 2. \tag{5}$$

Given Eq. (2)(3)(4)(5), the relationship between N and M is obtained as

$$N = (\alpha_S - 2) \cdot S_0 \cdot M^{\lambda}. \tag{6}$$

It combines a power-law component M^{λ} and a linear component $\alpha_S - 2$. From Fig. 3D, it is evident that the observed data aligns closely with the theoretical values ($R^2 = 0.96$).

It can be observed in Fig. 3D that as the travel demand increases, the number of jammed clusters also increases but at a steadily diminishing rate, similar to the sub-linear growth of S_{total}. This result indicates that the increase in travel demand initially leads to rapidly growing congestion when the road segments reach their capacity limit. However, as travel demand continuously increases, the growth rate of N slows down. One possible explanation is that as more congestion clusters occur, small clusters are more likely to merge and limit the total number of clusters. Moreover, noting that our analysis represents the congestion over a day, the temporal variations of travel demand may also contribute to the result. The growth in travel demand during peak periods may be more pronounced, leading to a sharp increase in N. However, residents may correspondingly adjust their travel periods to avoid peak, which results in a slowdown of congestion growth.

2.3 Scaling laws for the propagation of congestion

The linear relationship between demand and scaling exponents implies that travel demand directly influences the micro-mechanism of congestion cluster formation. Therefore, we examined the microscopic level of congestion propagation, aiming to enhance the understanding of this dynamic process.

To examine congestion in successive periods, we track the total number of congested roads, denoted as C, at five-minute intervals between 6:00 a.m. and 11:00 p.m. For fine-grained traffic demand, we calculate the total number of vehicles on the road network V corresponding to each time interval, using a moving average of three intervals for noise reduction. Unlike S_{total} and M for daily aggregation, C and V represent the congestion and demand at any given time slot respectively, forming the microscopic perspective of congestion. This facilitates a more detailed observation of the travel demand and congestion over consecutive periods.

Figure 4B illustrates the scatter plot of C versus V on double logarithmic axes, revealing an obvious power-law relation with the exponent γ of approximately 2.10 ($R^2 = 0.89, 95\% CI = [2.06, 2.12]$):

$$C = k \cdot V^{\gamma}. \tag{7}$$

Note that in contrast to the sub-linear scaling of S_{total} and M during the whole day, congested roads C increase with vehicles on road V with a super-linear scaling pattern, which means slight increases in travel demand can rapidly elevate the number of congested roads and exacerbate traffic congestion. It is also interesting that the scaling exponent γ falls between 2 and 3 for congested road networks, similar to other complex networks such as social networks [63–65], urban road networks [66, 67], and so on.

To further examine the cascading propagation of congestion, we differentiate C into three distinct components based on the real scenarios of traffic congestion and relevant literature: 1) congestion generated through cascade diffusion, denoted by F, which is the accumulation number of congested roads that are connected to pre-existing congestion; 2) congestion generated spontaneously, denoted by I, which is the accumulation number of congested roads that arise spontaneously; 3) dissipation, denoted by R, which is the accumulation number of roads that were congested but subsequently recovered. The distinction of C into diffusion (F), spontaneous congestion (I), and recovery (R) is based on real scenarios. Typical congestion would start from a spontaneously congested road (I) associated with sporadic factors such as traffic accidents and construction projects [1, 68, 69]. Then, the congestion would diffuse (F) with traffic flow and road network topology, which may persist for extended periods during peak hours [23, 70]. Finally, the congested roads

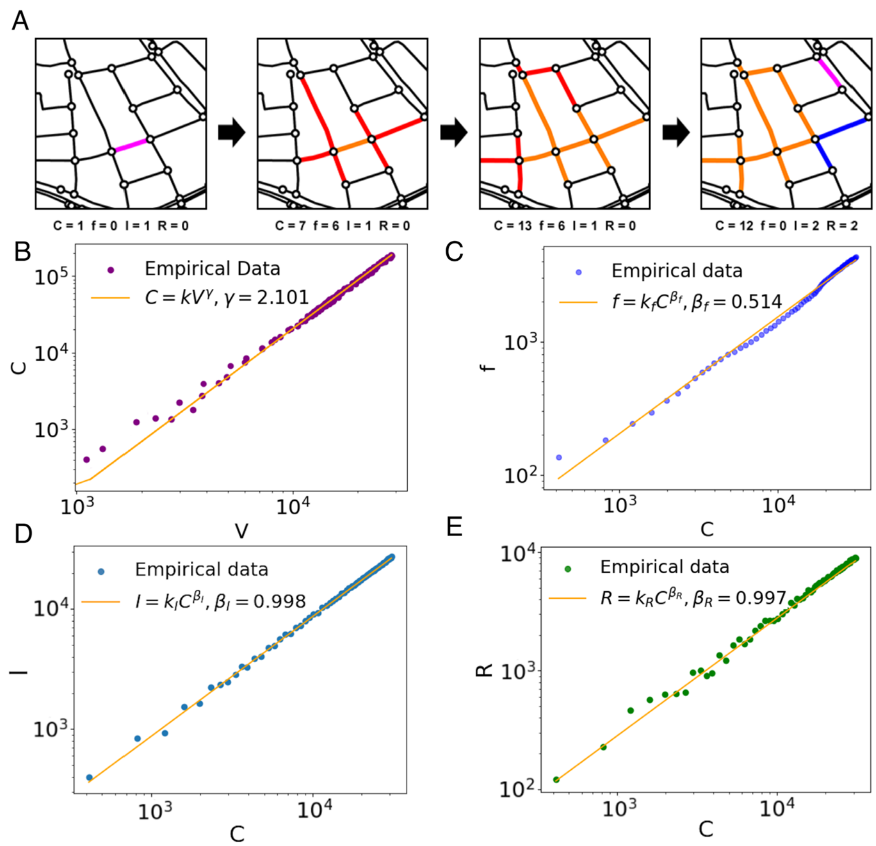

Figure 4 Power law relationship of road congestion on March 1st in Shanghai. (A) A demonstration of cascading progress in the traffic network. Color represents the state of road segments, including spontaneous congestion (pink), cascading diffusion (red), existing congestion (orange), and dissipation (blue). (B) Power-law relationship between the total number of congested roads C and the travel demand V (represented by the number of vehicles recorded) in consecutive periods. (C) Illustration of the scaling relationship between the number of congested roads generated by diffusion, denoted as f and the total number of congested roads C. (D) Illustration of the scaling relationship between the number of spontaneously generated congested roads I and the total number of congested roads C. (E) Illustration of the scaling relationship between the number of dissipating roads R and the total number of congested roads C

will gradually recover (F), reflecting the self-healing capability of the transportation system. Traffic congestion exhibits such dynamic spatiotemporal patterns, and analyzing the temporal and spatial changes of different types of congestion helps provide a more comprehensive understanding of congestion patterns. This, in turn, allows for a more precise determination of measures needed to alleviate congestion. Figure 4A illustrates a sample of cascading progress and the corresponding components. Naturally, the sum of these three parts equals C:

$$C = F + I - R. \tag{8}$$

Since the diffusion component F is an extension from pre-existing congestion and inherently has an incremental property, we reformulate it using the newly added diffusive congested roads, denoted by f. The f directly captures the propagation rate of congestion at a given time, offering more information about congestion [4, 71–73]. The equation can be reformulated as:

$$C = \sum f + I - R, \tag{9}$$

We then examined the relationship between C and its three components f,I,R from our empirical data (Fig. 4C,D,E). The results show that all three components show a power law to the total number of congested roads on any given day.

$$f = k_f C^{\beta_f}, \qquad I = k_I C^{\beta_I}, \qquad R = k_R C^{\beta_R}. \tag{10}$$

Taking data on March 1st as an example, results shows that f obeys sub-linear growth to C with $\beta_f = 0.514 \pm 0.011, (R^2 = 0.92)$. While I and R is approximately linear to C with $\beta_I = 0.998 \pm 0.003, (R^2 = 0.88)$ and $\beta_R = 0.997 \pm 0.007, (R^2 = 0.89)$. The result is stable over different dates and travel demand (refer to Additional File 1, Sect. 5 for more information).

The results show that both I and R demonstrate almost linear relationships with C, meaning they keep proportional to C despite dates and demand. For spontaneously generated component I that serves as seeds of congestion clusters, this proportion can be related to relatively stable road capacity and recurring congestion [74]. Regarding the dissipation component R, the constant proportion suggests the dissipation is independent of present congestion and can be simply described by a dissipation rate [3]. As for the sub-linear scaling of diffusion f, one plausible conjecture is that the network topology may impose constraints besides the intrinsic diffusion dynamics, similar to what has been observed in urban amenities [42, 67]. Further investigation into the topology structure may provide more insight into it.

Based on the existing results, we examine how the three components determine the power-law relationship of C and V by determining key coefficients k and γ. Starting with the difference in congested roads in different demand scenarios, we have a differential form of the congestion propagation:

$$\frac{dC}{dV} = f + \frac{dI}{dV} - \frac{dR}{dV}. \tag{11}$$

While Eq. (11) cannot be solved for an analytic expression, an approximation can still be derived under the empirical data showing $\beta_I \approx 1$ and $\beta_R \approx 1$. Based on Eq. (10), (11), we can obtain

$$k \approx \frac{k_f(1-\beta_f)}{1-k_I+k_R}, \gamma \approx \frac{1}{1-\beta_f}, \tag{12}$$

with both k and γ are determined by the coefficients and exponents of components (See Additional File 1 Sect. 4 for more information).

Figure 5A,B,C show that the values of β_f, β_I, and β_R exhibit relatively stable distributions in all observed days ($\beta_f = 0.515 \pm 0.002$, $\beta_I = 0.996 \pm 0.002$, $\beta_R = 0.996 \pm 0.002$). Considering the drastic changes in daily demand M, the observation suggests a universal connection in congestion components over consecutive time. The observed empirical data of k and γ is illustrated in Fig. 5D,E, alongside their corresponding theoretical values obtained through Eq. (12). Notably, Eq. (12) indicates that both k and γ are solely correlated with β_f, demonstrating the dominant role of cascade diffusion in the growth of

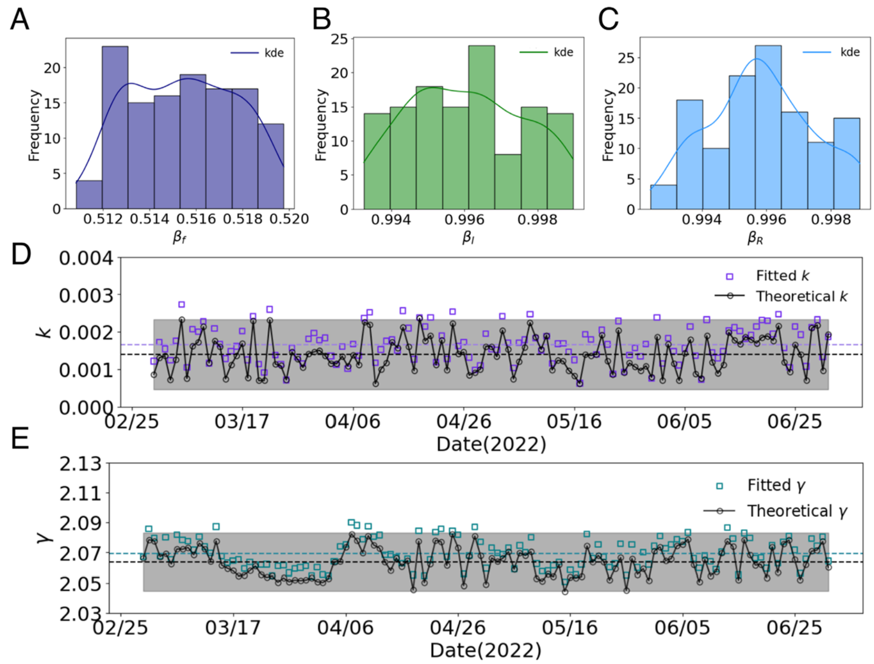

Figure 5 Distribution of fitted exponents for the 123 different days and the theoretical and empirical values for k and γ as a function of date. (A) Distribution of the scaling exponent β_f with kernel density estimation. (B) Distribution of the scaling exponent β_l with kernel density estimation. (C) Distribution of the scaling exponent β_R with kernel density estimation. (D) The theoretical (gray) and empirical (purple) values of k as a function of date. The shadow areas represent the 95%CI of k. (E) The theoretical (gray) and empirical (blue) values of γ as a function of date. The shadow areas represent the 95%CI of γ

congestion. The reciprocal-like relationship between γ and β_f demonstrates how a sub-linear growth of cascading diffusion leads to super-linear growth of total congested roads. These scaling laws enable us to comprehend the micro-scale mechanism underlying congestion across different travel demand, making it conceivable that universally applicable strategies for congestion management may exist.

3 Discussion

Traffic demand has always been one of the key factors when examining traffic congestion [10–15]. Our primary contribution lies in discovering a universal scaling law that constrains the spatiotemporal scale and propagation patterns of congestion in cities under varying travel demand. In this research, we identify the crucial role of travel demand in the scaling laws of urban traffic congestion. Based on the real traffic data during the COVID-19 pandemic in Shanghai, we extend our research on the power-law scaling of urban traffic congestion and reveal the relationship between traffic congestion and travel demand at the macroscopic congestion cluster and the microscopic congestion propagation.

Compared to the study by Zhang et al. [53], we have utilized more recent traffic data to verify the power-law distribution in scenarios with varied traffic demand. Our results illustrate that changes in traffic demand directly affect traffic resilience, with a negative linear relationship that has not been reported before. Such results suggest that congestion can be predicted and intervened by managing travel demand, and proper mitigation resources and policies should be designed for different demand levels. Furthermore, the sub-linear power-law relationship between traffic demand and the total congestion size demonstrates resilience within the transportation system [75]. More efficient and frugal methods and policies could be developed under the guidance of such resilience. It is also interesting that the scaling exponent γ, between the number of congested roads and the number of vehicles, falls between 2 and 3. One of the possible explanations is the preferential attachment mechanism commonly used to model a dynamic network. A small fraction of congestion bottlenecks within the traffic network attracted newly congested segments driven by demand, establishing the super-linear growth pattern. The initial bottlenecks and subsequent attachments form the cascading propagation. Although we have not conducted any direct analysis to support such a hypothesis, we believe that future modeling based on it may provide a detailed analysis of the internal mechanisms.

At the micro level, the super-linear growth pattern of congested roads highlights the potential of significant congestion arising from minor increases in travel demand, in line with the cascading dynamics of congestion [58]. Using the cascading failure framework [4], we discover a stable proportion of spontaneous generation and dissipation across dates and demand levels, implying it can be hard to ease congestion by speeding dissipation or reducing spontaneous generation. However, the sub-linear scaling relation between diffusion and congested roads indicates that diffusion increases relatively slower, and blocking cascading diffusion through appropriate early intervention could be an essential path to avoid cascading diffusion and change congestion distribution. Our result is of great theoretical interest since it can link the cascade diffusion to the scaling law framework and illustrate that the cascade diffusion rate is decisive to the power-law of congestion.

The two distinct power-law growth exponents we have observed at the cluster level and road level hold significant implications. Although total congestion cluster size is sublinearly scaling with daily travel demand, the congested road number is a super-linear scaling to short-term travel demand. Similar paradoxical scaling laws have been found in other areas of urban research [76]. For instance, there is a sub-linear or linear relationship between building area and population in various administrative districts of Shanghai. However, a super-linear scaling law emerges between building area and population among more administrative districts over time [77]. Studies have also revealed that different scaling relationships can arise due to variations in the definition of cities [78–80] or differences among groups [81]. This difference means we should consider targeted measurements and management on different space or time scales.

Specifically, the sub-linear growth at the daily clusters suggests that people have more flexibility and adaptability to avoid peak hours by choosing alternative transportation modes or changing their schedules, resulting in a lower growth rate than the travel demand. Therefore, it is essential to consider people's flexibility and adaptability for long-term planning to alleviate traffic pressure. Persistent measures like encouraging alternative transportation choices, optimizing public transportation systems, and implementing differentiated road tolls help alleviate overall congestion pressure and ensure efficient, safe, and sustainable urban transportation development. However, the super-linear growth within consecutive time intervals is related to the cascade diffusion, leading to the rapid emergence of road bottlenecks and congestion spread. Hence, short-term response and quick interventions are necessary, including monitoring fluctuations in traffic flow on highly connected roads and promptly identifying potential bottlenecks. Such distinct managing strategies are based on the different characteristics in different time scales, leading to distinct traffic optimization directions.

Regarding the observed power-law growth pattern of congestion with traffic demand, our data only provide observations from one city focusing on the demand changes. Due to constraints related to data availability and research resources, our research exclusively utilized traffic data from Shanghai during the COVID-19 pandemic. Unlike minor fluctuations in traffic demand under normal conditions, this unique dataset provided us with an opportunity to investigate congestion patterns throughout the entire process of a significant decrease in traffic demand to recovery, thereby establishing a link between traffic demand and congestion. With more urban data, we can verify if similar congestion patterns exist in other cities in future work. Besides, although we utilized data including the period before the lockdown (March 1st to March 28th) and after the lockdown (June 1st to July 1st), the COVID-19 pandemic may have drastically altered our cities and making the comparison using multi-year historical data an important aspect. Furthermore, the authorities implemented traffic control measures like checkpoints during the lockdown, which could potentially impact the occurrence and propagation of traffic congestion. Although most lockdown policies are mainly achieved by reducing travel demand, which is covered in our study, the subsequent effect on other aspects, like travel mode preference [82], should be carefully examined in the future. Other factors, such as road network topology and traffic flow heterogeneity, can also be included to describe the congestion dynamics. Unexpected weather conditions, road incidents, ongoing construction, and road capacity can all affect the relationship between travel demand and traffic congestion. In future research, our analytical framework can be extended to encompass a broader range of urban contexts, enabling its application to multiple cities. It is promising that big traffic data will continue to enhance our understanding of traffic congestion and contribute to effective strategies for managing transportation systems.

4 Materials and methods

4.1 Traffic dataset

Our research is primarily based on travel Origin-Destination (OD) data and road congestion index data (0 for congested, and 1 for normal traffic flow) with a resolution of 5 min in Shanghai. The dataset covers a time period of 123 days from March 1st to June 1st, 2022, collected through floating car records in Shanghai. The data are sourced from a large map service provider. In addition, we have collected topological data on the road network of Shanghai from the OpenStreetMap [83], which includes the adjacency relations among major roads in Shanghai. The dataset contains over 32,000 road segments, along with the lists of outbound and inbound roads for each segment.

4.2 Definition of spatiotemporal jammed clusters

Based on the topological information of the road network in Shanghai, we define a spatial-temporal network G_T. G is a directed connected graph, representing a snapshot of the graph at time T. And T is a period comprising a set of consecutive time slots. The edges in E represent road segments and the nodes in V represent the adjacencies of the road segments. The direction of edges is the same as the direction of congestion propagation, and the opposite direction of traffic flow. In the first snapshot, denoted as t_0, all connected road segments form the initial jammed cluster. For each subsequent snapshot t, the newly

Table 1 List of Symbols and Description

Symbol	Description	Symbol	Description
S	Cluster size	α_S	Scaling exponent of S
T	Recovery Duration	α_T	Scaling exponent of T
M	Total daily travel demand	S_{total}	Total number of cluster size
N	Daily number of jammed clusters	V	Travel demand represented by vehicles on the road
C	The total number of congested roads	γ	Scaling exponent of C
k	Normalization constant of C	F	Number of congested roads due to diffusion
f	Number of newly-added diffusive congested roads	β_f	Scaling exponent of f
I	Number of spontaneously generated congested roads	β_I	Scaling exponent of I
R	Number of dissipating roads	β_R	Scaling exponent of R

congested road segments connected to the previous snapshot are grouped into the same jammed cluster. Within the time period from t_0 to t_n, congested and connected road segments are included in the same jammed cluster. Therefore, the jammed cluster at snapshot t represents the spatio-temporal distribution of road congestion at time t. It should be noted that if two jammed clusters are connected during the diffusion process, they are considered as the same jammed cluster. Ultimately, multiple jammed clusters are obtained within the time period from t_0 to t_n, representing the distribution of congestion throughout the day (refer to Additional File 1, Sect. 2 for detailed definition). The full list of symbols is shown in Table 1.

4.3 Parameter fitting methods

The fitting of the power-law distribution is accomplished through the powerlaw package [84] in Python. We used the ordinary least square (OLS) method to fit the data and estimated parameters of the power function as previous literature [53, 85]. The power function is defined as $y = ax^b$, where a and b are parameters, x is the independent variable, and y is the dependent variable. The principle of fitting involves minimizing the error between the power function and real data utilizing ordinary least squares estimation.

$$\min_{a,b} \sum_i \bigl(\log(y_i) - b\log(x_i) - \log(a)\bigr)^2. \tag{13}$$

The selection of OLS method is grounded in the minimal variance and absence of heterogeneous fluctuations in our dataset, where OLS reliably delivers reasonable and easily interpretable outcomes. However, in scenarios characterized by substantial variance and heteroscedasticity, alternative methods such as probabilistic models [86] ought to be explored. Please refer to Additional File 1, Sect. 3 for more details.

Supplementary information

Supplementary information accompanies this paper at https://doi.org/10.1140/epjds/s13688-024-00471-4.

Additional file 1. We report additional details on methods and results. (PDF 204 kB)

Acknowledgements
Not applicable.

Author contributions
R. Chen, Y. Lin, H. Yan and Y. Li conceived the idea and designed the experiments; R. Chen and Y. Lin analyzed the data and performed the experiments; R. Chen, Y. Lin and Y. Li wrote the paper. All authors reviewed and edited the paper.

Funding
Supported by the National Natural Science Foundation of China (Grant No. 62302261).

Data availability
The data that support the findings of this study are available from Amap-Alibaba Group but restrictions apply to the availability of these data, which were used under license for the current study, and so are not publicly available. Data are however available from the authors upon reasonable request and with permission of Amap-Alibaba Group.

Declarations

Competing interests
The authors declare that they have no competing interests.

Received: 12 September 2023 Accepted: 3 April 2024 Published online: 11 April 2024

References

1. Li D, Fu B, Wang Y, Lu G, Berezin Y, Stanley HE, Havlin S (2015) Percolation transition in dynamical traffic network with evolving critical bottlenecks. Proc Natl Acad Sci 112(3):669–672
2. Bob P (2022) inrix global traffic scorecard. Technical report, INRIX Research (2023)
3. Saberi M, Hamedmoghadam H, Ashfaq M, Hosseini SA, Gu Z, Shafiei S, Nair DJ, Dixit V, Gardner L, Waller ST et al (2020) A simple contagion process describes spreading of traffic jams in urban networks. Nat Commun 11(1):1616
4. Duan J, Li D, Huang H-J (2023) Reliability of the traffic network against cascading failures with individuals acting independently or collectively. Transp Res, Part C, Emerg Technol 147:104017
5. Xiong H, Vahedian A, Zhou X, Li Y, Luo J (2018) Predicting traffic congestion propagation patterns: a propagation graph approach. In: Proceedings of the 11th ACM SIGSPATIAL international workshop on computational transportation science, pp 60–69
6. Wang Z, Xie S, Ouyang Y (2022) Planning reliable service facility location against disruption risks and last-mile congestion in a continuous space. Transp Res, Part B, Methodol 165:123–140
7. Loo BP, Huang Z (2022) Spatio-temporal variations of traffic congestion under work from home (wfh) arrangements: lessons learned from Covid-19. Cities 124:103610
8. Baldi S, Michailidis I, Ntampasi V, Kosmatopoulos E, Papamichail I, Papageorgiou M (2019) A simulation-based traffic signal control for congested urban traffic networks. Transp Sci 53(1):6–20
9. Li X, Yang H, Ke J (2023) Booking cum rationing strategy for equitable travel demand management in road networks. Transp Res, Part B, Methodol 167:261–274
10. Batarce M, Ivaldi M (2014) Urban travel demand model with endogenous congestion. Transp Res, Part A, Policy Pract 59:331–345
11. Metz D (2010) Saturation of demand for daily travel. Transp Rev 30(5):659–674
12. Wisetjindawat W, Derrible S, Kermanshah A (2018) Modeling the effectiveness of infrastructure and travel demand management measures to improve traffic congestion during typhoons. Transp Res Rec 2672(1):43–53
13. Zhou Z, Roncoli C (2022) A scalable vehicle assignment and routing strategy for real-time on-demand ridesharing considering endogenous congestion. Transp Res, Part C, Emerg Technol 139:103658
14. Toole JL, Colak S, Sturt B, Alexander LP, Evsukoff A, González MC (2015) The path most traveled: travel demand estimation using big data resources. Transp Res, Part C, Emerg Technol 58:162–177
15. Bigazzi AY, Figliozzi MA (2012) Congestion and emissions mitigation: a comparison of capacity, demand, and vehicle based strategies. Transp Res, Part D, Transp Environ 17(7):538–547
16. Çolak S, Lima A, González MC (2016) Understanding congested travel in urban areas. Nat Commun 7(1):10793
17. Handy S, Boarnet MG (2014) Impact of highway capacity and induced travel on passenger vehicle use and greenhouse gas emissions. California Environmental Protection Agency, Air Resources Board, Retrieved August 28, 2015
18. Cheng Z, Pang M-S, Pavlou PA (2020) Mitigating traffic congestion: the role of intelligent transportation systems. Inf Syst Res 31(3):653–674
19. Lam WH, Shao H, Sumalee A (2008) Modeling impacts of adverse weather conditions on a road network with uncertainties in demand and supply. Transp Res, Part B, Methodol 42(10):890–910
20. Sun H, Wu J, Ma D, Long J (2014) Spatial distribution complexities of traffic congestion and bottlenecks in different network topologies. Appl Math Model 38(2):496–505
21. Tsuzuki S, Yanagisawa D, Nishinari K (2022) Effect of congestion avoidance due to congestion information provision on optimizing agent dynamics on an endogenous star network topology. Sci Rep 12(1):22159
22. Menelaou C, Timotheou S, Kolios P, Panayiotou CG, Polycarpou MM (2018) Minimizing traffic congestion through continuous-time route reservations with travel time predictions. IEEE Trans Intell Veh 4(1):141–153
23. Wong W, Wong S (2016) Network topological effects on the macroscopic bureau of public roads function. Transportmetrica A: Transp Sci 12(3):272–296
24. Nguyen-Phuoc DQ, Currie G, De Gruyter C, Young W (2018) Exploring the impact of public transport strikes on travel behavior and traffic congestion. Int J Sustain Transp 12(8):613–623
25. Aftabuzzaman M (2007) Measuring traffic congestion-a critical review. In: 30th Australasian transport research forum. ETM GROUP, London, pp 1–16
26. Jansson JO (2008) Public transport policy for central-city travel in the light of recent experiences of congestion charging. Res Transp Econ 22(1):179–187
27. Albert G, Mahalel D (2006) Congestion tolls and parking fees: a comparison of the potential effect on travel behavior. Transp Policy 13(6):496–502
28. Metz D (2012) Demographic determinants of daily travel demand. Transp Policy 21:20–25

29. Moyano A, Stępniak M, Moya-Gómez B, García-Palomares JC (2021) Traffic congestion and economic context: changes of spatiotemporal patterns of traffic travel times during crisis and post-crisis periods. Transportation 48(6):3301–3324
30. Hahn E, Chatterjee A, Sue Younger M (2002) Macro-level analysis of factors related to areawide highway traffic congestion. Transp Res Rec 1817(1):11–16
31. Kim TJ (1983) A combined land use-transportation model when zonal travel demand is endogenously determined. Transp Res, Part B, Methodol 17(6):449–462
32. Kuzmyak JR (2012) Land use and traffic congestion. Technical report, Arizona. Dept. of Transportation, Research Center
33. McNally MG, Kulkarni A (1997) Assessment of influence of land use–transportation system on travel behavior. Transp Res Rec 1607(1):105–115
34. Anas A, Xu R (1999) Congestion, land use, and job dispersion: a general equilibrium model. J Urban Econ 45(3):451–473
35. Suarez P, Anderson W, Mahal V, Lakshmanan T (2005) Impacts of flooding and climate change on urban transportation: a systemwide performance assessment of the Boston metro area. Transp Res, Part D, Transp Environ 10(3):231–244
36. Pei Y, Cai X, Li J, Song K, Liu R (2021) Method for identifying the traffic congestion situation of the main road in cold-climate cities based on the clustering analysis algorithm. Sustainability 13(17):9741
37. Simic V, Gokasar I, Deveci M, Švadlenka L (2022) Mitigating climate change effects of urban transportation using a type-2 neutrosophic merec-marcos model. IEEE Trans Eng Manag
38. Zeng G, Li D, Guo S, Gao L, Gao Z, Stanley HE, Havlin S (2019) Switch between critical percolation modes in city traffic dynamics. Proc Natl Acad Sci 116(1):23–28
39. Hamedmoghadam H, Jalili M, Vu HL, Stone L (2021) Percolation of heterogeneous flows uncovers the bottlenecks of infrastructure networks. Nat Commun 12(1):1254
40. Batty M (2008) The size, scale, and shape of cities. Science 319(5864):769–771
41. Bettencourt LM, Lobo J, Helbing D, Kühnert C, West GB (2007) Growth, innovation, scaling, and the pace of life in cities. Proc Natl Acad Sci 104(17):7301–7306
42. Kaufmann T, Radaelli L, Bettencourt LM, Shmueli E (2022) Scaling of urban amenities: generative statistics and implications for urban planning. EPJ Data Sci 11(1):50
43. Schläpfer M, Bettencourt LM, Grauwin S, Raschke M, Claxton R, Smoreda Z, West GB, Ratti C (2014) The scaling of human interactions with city size. J R Soc Interface 11(98):20130789
44. Taillanter E, Barthelemy M (2021) Empirical evidence for a jamming transition in urban traffic. J R Soc Interface 18(182):20210391
45. Wang R, Wang Q, Li N (2023) Percolation transitions in urban mobility networks in America's 50 largest cities. Sustain Cities Soc 91:104435. https://doi.org/10.1016/j.scs.2023.104435
46. Barabási A-L (2009) Scale-free networks: a decade and beyond. Science 325(5939):412–413
47. Goh K-I, Oh E, Jeong H, Kahng B, Kim D (2002) Classification of scale-free networks. Proc Natl Acad Sci 99(20):12583–12588
48. Kempes CP, Koehl M, West GB (2019) The scales that limit: the physical boundaries of evolution. Front Ecol Evol 7:242
49. West GB, Brown JH, Enquist BJ (2001) A general model for ontogenetic growth. Nature 413(6856):628–631
50. Kempes CP, Dutkiewicz S, Follows MJ (2012) Growth, metabolic partitioning, and the size of microorganisms. Proc Natl Acad Sci 109(2):495–500
51. Baiesi M, Paczuski M (2004) Scale-free networks of earthquakes and aftershocks. Phys Rev E 69(6):066106
52. Li L, Doyle JC, Willinger W, Alderson D (2005) Towards a theory of scale-free graphs: definition, properties, and implications. Internet Math 2(4)
53. Zhang L, Zeng G, Li D, Huang H-J, Stanley HE, Havlin S (2019) Scale-free resilience of real traffic jams. Proc Natl Acad Sci 116(18):8673–8678
54. Wu AY, Garland M, Han J (2004) Mining scale-free networks using geodesic clustering. In: Proceedings of the tenth ACM SIGKDD international conference on knowledge discovery and data mining, pp 719–724
55. Zhou B, Meng X, Stanley HE (2020) Power-law distribution of degree–degree distance: a better representation of the scale-free property of complex networks. Proc Natl Acad Sci 117(26):14812–14818
56. Park K, Lai Y-C, Ye N (2005) Self-organized scale-free networks. Phys Rev E 72(2):026131
57. Haruna T, Gunji Y-P (2019) Ordinal preferential attachment: a self-organizing principle generating dense scale-free networks. Sci Rep 9(1):4130
58. Bellocchi L, Geroliminis N (2020) Unraveling reaction-diffusion-like dynamics in urban congestion propagation: insights from a large-scale road network. Sci Rep 10(1):4876
59. Wang M, Debbage N (2021) Urban morphology and traffic congestion: longitudinal evidence from us cities. Comput Environ Urban Syst 89:101676
60. Wei Y, Wang J, Song W, Xiu C, Ma L, Pei T (2021) Spread of Covid-19 in China: analysis from a city-based epidemic and mobility model. Cities 110:103010
61. Tian H, Liu Y, Li Y, Wu C-H, Chen B, Kraemer MU, Li B, Cai J, Xu B, Yang Q et al (2020) An investigation of transmission control measures during the first 50 days of the Covid-19 epidemic in China. Science 368(6491):638–642
62. Zhai Y, Han G (2023) Lockdown, information quality, and political trust: an empirical study of the shanghai lockdown under covid-19. Int Rev Adm Sci 00208523231166254
63. Arenas A, Danon L, Diaz-Guilera A, Gleiser PM, Guimera R (2004) Community analysis in social networks. Eur Phys J B 38:373–380
64. Wei Z, Wu H, Yuan X, Huang S, Feng Z (2017) Achievable capacity scaling laws of three-dimensional wireless social networks. IEEE Trans Veh Technol 67(3):2671–2685
65. Chowell G, Hyman JM, Eubank S, Castillo-Chavez C (2003) Scaling laws for the movement of people between locations in a large city. Phys Rev E 68(6):066102
66. Lämmer S, Gehlsen B, Helbing D (2006) Scaling laws in the spatial structure of urban road networks. Phys A, Stat Mech Appl 363(1):89–95

67. Molinero C, Thurner S (2021) How the geometry of cities determines urban scaling laws. J R Soc Interface 18(176):20200705
68. Quddus MA, Wang C, Ison SG (2010) Road traffic congestion and crash severity: econometric analysis using ordered response models. J Transp Eng 136(5):424–435
69. Long J, Gao Z, Ren H, Lian A (2008) Urban traffic congestion propagation and bottleneck identification. Sci China, Ser F, Inf Sci 51(7):948–964
70. Wu C-Y, Hu M-B, Jiang R, Hao Q-Y (2021) Effects of road network structure on the performance of urban traffic systems. Phys A, Stat Mech Appl 563:125361
71. Hamedmoghadam H, Zheng N, Li D, Vu HL (2022) Percolation-based dynamic perimeter control for mitigating congestion propagation in urban road networks. Transp Res, Part C, Emerg Technol 145:103922
72. Duan D, Lv C, Si S, Wang Z, Li D, Gao J, Havlin S, Stanley HE, Boccaletti S (2019) Universal behavior of cascading failures in interdependent networks. Proc Natl Acad Sci 116(45):22452–22457
73. Daqing L, Yinan J, Rui K, Havlin S (2014) Spatial correlation analysis of cascading failures: congestions and blackouts. Sci Rep 4(1):5381
74. Kumar N, Raubal M (2021) Applications of deep learning in congestion detection, prediction and alleviation: a survey. Transp Res, Part C, Emerg Technol 133:103432
75. Salat S (2017) A systemic approach of urban resilience: power laws and urban growth patterns. Int J Urban Sustain Dev 9(2):107–135
76. Bettencourt LM, Yang VC, Lobo J, Kempes CP, Rybski D, Hamilton MJ (2020) The interpretation of urban scaling analysis in time. J R Soc Interface 17(163):20190846
77. Xu G, Xu Z, Gu Y, Lei W, Jiao L (2020) Scaling laws in intra-urban systems and over time at the district level in Shanghai, China. Phys A, Stat Mech Appl 125162
78. Louf R, Barthelemy M (2014) Scaling: lost in the smog. Environ Plan B, Plan Des 41(5):767–769
79. Arcaute E, Hatna E, Ferguson P, Youn H, Johansson A, Batty M (2015) Constructing cities, deconstructing scaling laws. J R Soc Interface 12(102):20140745
80. Cottineau C, Hatna E, Arcaute E, Batty M (2017) Diverse cities or the systematic paradox of urban scaling laws. Comput Environ Urban Syst 63:80–94
81. Strano E, Sood V (2016) Rich and poor cities in Europe. An urban scaling approach to mapping the European economic transition. PLoS ONE 11(8):0159465
82. Abdullah M, Dias C, Muley D, Shahin M (2020) Exploring the impacts of Covid-19 on travel behavior and mode preferences. Transp Res Interdiscip Perspect 8:100255. https://doi.org/10.1016/j.trip.2020.100255
83. OpenStreetMap contributors (2017) Planet dump retrieved from https://planet.osm.org. https://www.openstreetmap.org
84. Alstott J, Bullmore E, Plenz D (2014) Powerlaw: a python package for analysis of heavy-tailed distributions. PLoS ONE 9(1):85777
85. Clauset A, Shalizi CR, Newman ME (2009) Power-law distributions in empirical data. SIAM Rev 51(4):661–703
86. Leitão JC, Miotto JM, Gerlach M, Altmann EG (2016) Is this scaling nonlinear? R Soc Open Sci 3(7):150649. https://doi.org/10.1098/rsos.150649

Publisher's Note

Springer Nature remains neutral with regard to jurisdictional claims in published maps and institutional affiliations.